An Investigation of the Structures, Vibrational Spectra, and Relative Energetics of CH_3COBrO_3 Isomers

Sujata Guha and Joseph S. Francisco*

Department of Chemistry and Department of Earth & Atmospheric Sciences, Purdue University, West Lafayette, Indiana 47907-1393

Received: October 18, 2000; In Final Form: January 26, 2001

The structures, vibrational spectra, and relative energetics of CH_3COBrO_3 isomers have been examined using the B3LYP method in conjunction with different basis sets. The $CH_3COOBrO_2$ structural form is found to possess the lowest energy with an estimated heat of formation of -38.2 kcal mol^{-1}, at 0 K, as determined from G2MP2 theory. The next lowest energy structural form is $CH_3COOOOBr$, which lies 7.7 kcal mol^{-1} above $CH_3COOBrO_2$. The isomeric forms possessing higher energies are $CH_3COOOBrO$ and CH_3COBrO_3. We have examined the implication of the formation of CH_3COBrO_3 isomers from the atmospheric cross-reactions of the acetylperoxy (CH_3COO_2) and bromine monoxide (BrO) radicals and determined the possible dissociation products of the most likely CH_3COBrO_3 isomers.

I. Introduction

Bromine is the most effective halogen that participates in efficient catalytic cycles leading to the destruction of stratospheric ozone. Although bromine-containing compounds are much less abundant than chlorine-containing compounds in the stratosphere, it has been estimated that the chemistry involving bromine species is responsible for ~25% of the loss of ozone in Antarctica[1] and up to 40% of ozone loss during winter in the Arctic region.[2] The efficiency of bromine in destroying the ozone layer is greatly enhanced by its synergistic coupling with chlorine compounds, leading to the production of bromine and chlorine atoms.[3]

$$BrO + ClO \rightarrow Br + Cl + O_2 \qquad (1)$$

The most abundant bromine-containing source gas is methyl bromide (CH_3Br), present mainly due to oceanic biological processes. Methyl bromide is used for fumigation purposes, has a high ozone depletion potential (ODP), and is scheduled to be phased out in developed countries by the year 2010.[4] Other important source gases of bromine that reach the stratosphere after emission from the troposphere include tetrabromobisphenol A and trifluoromethyl bromide, used as fire retardants and refrigerants.

The coupling of bromine oxides with other radical families in the atmosphere is critical to the destruction of the ozone layer. An important coupling reaction occurs between the HO_x and BrO_x families, specifically between HO_2 and BrO radicals. This reaction leads to the primary production of hypobromous acid (HOBr) and determines the concentration of ozone in the stratosphere.[5−17]

$$HO_2 + BrO \rightarrow HOBr + O_2 \qquad (2)$$

Similar to the HO_2 + BrO reaction is the CH_3O_2 + BrO reaction, which has been thought to be involved in the bromine-catalyzed oxidation of methane, as speculated in a modeling study of the chemistry of the lower stratosphere. The CH_3O_2 + BrO reaction has also been considered in catalytic cycles which could result from bromine being released from sea salt aerosols in the marine boundary layer.[18] The following pathways have been considered for the reaction between CH_3O_2 and BrO radicals.

$$CH_3O_2 + BrO \rightarrow HOBr + CH_2O_2 \qquad (3a)$$

$$\rightarrow Br + CH_3O + O_2 \qquad (3b)$$

$$\rightarrow OBrO + CH_3O \qquad (3c)$$

$$\rightarrow HBr + CH_2O + O_2 \qquad (3d)$$

$$\rightarrow CH_3OBr + O_2 \qquad (3e)$$

Aranda et al.[18] used discharge flow-mass spectrometry with laser-induced fluorescence to study the kinetics of the CH_3O_2 + BrO reaction and postulated that CH_3OBr, formed in channel 3e, would be of minor importance. They stated that the reaction between CH_3O_2 and BrO radicals is likely to be negligible in the stratosphere, but is potentially significant in the marine boundary layer and can affect the flora and fauna of that region. Guha and Francisco[19] performed computations on the possible $CH_3O_2\cdots BrO$ complexes that could be formed from the coupling between CH_3O_2 and BrO radicals, and determined their structural, spectroscopic, and energetic properties.

Similar to the reaction between CH_3O_2 and BrO radicals, a reaction could occur between CH_3COO_2 and BrO radicals in the stratosphere. CH_3COO_2, also known as acetylperoxy radicals, are formed due to the three-body recombination reaction of CH_3CO radicals, produced from the reaction between acetaldehyde (CH_3CHO) and hydroxyl radicals.[20,21]

$$CH_3CHO + OH \rightarrow CH_3CO + H_2O \qquad (4)$$

$$CH_3CO + O_2 + M \rightarrow CH_3COO_2 + M \qquad (5)$$

In this paper we have examined the possibility of existence of the different $CH_3COO_2\cdots BrO$ (or CH_3COBrO_3) complexes during the reaction between CH_3COO_2 and BrO radicals. We have also examined the possible dissociation products of the

10.1021/jp0038409 CCC: \$20.00

TABLE 1: Optimized Geometries (Å and Deg) of CH_3COBrO_3 Isomers

		levels of theory B3LYP/				
species	coordinates	6-31G(d)	6-311G(d,p)	6-311G(2d,2p)	6-311G(2df,2p)	6-311++G(3df,3pd)
$CH_3COO'OOBr$	*r*(CO)	1.196	1.189	1.188	1.187	1.188
	r(CO′)	1.395	1.396	1.395	1.392	1.392
	r(CC)	1.511	1.508	1.506	1.505	1.504
	r(OO)	1.355	1.340	1.351	1.355	1.355
	r(O′O)	1.464	1.467	1.458	1.452	1.451
	r(OBr)	1.941	1.965	1.941	1.918	1.912
	r(CH)	1.091	1.089	1.085	1.085	1.086
	r(CH′)	1.094	1.090	1.088	1.089	1.088
	r(CH″)	1.095	1.093	1.090	1.090	1.090
	∠(CO′O)	110.9	111.5	111.0	111.2	111.5
	∠(CCO)	128.0	128.1	128.0	128.1	127.9
	∠(CCO′)	107.5	107.4	107.6	107.5	107.7
	∠(O′OO)	108.5	109.2	108.8	108.7	108.6
	∠(HCC)	108.4	108.4	108.4	108.5	108.5
	∠(H′CC)	111.0	111.6	111.1	110.7	111.3
	∠(H″CC)	109.7	108.7	109.3	109.8	109.0
	∠(OOBr)	111.4	112.5	111.8	111.9	112.0
	∠(HCCO)	9.3	23.3	13.4	6.0	15.8
	∠(H′CCO)	121.3	145.6	135.0	127.1	137.7
	∠(H″CCO)	−119.6	−95.0	−105.9	−114.0	−103.3
	∠(OCO′O)	−1.7	−0.8	−1.3	−1.9	−0.8
	∠(CO′OO)	83.3	83.2	83.0	84.1	85.0
	∠(O′OOBr)	84.2	84.9	85.1	85.2	85.1
$CH_3COO'OBrO'$	*r*(CO)	1.203	1.195	1.193	1.194	1.193
	r(CO′)	1.386	1.387	1.381	1.385	1.383
	r(CC)	1.506	1.503	1.502	1.503	1.501
	r(O′O)	1.422	1.416	1.424	1.421	1.422
	r(CH)	1.093	1.090	1.087	1.087	1.087
	r(CH′)	1.091	1.089	1.086	1.086	1.086
	r(CH″)	1.096	1.093	1.091	1.091	1.091
	r(OBr)	1.961	1.969	1.913	1.945	1.905
	r(BrO′)	1.689	1.684	1.661	1.674	1.662
	∠(CCO)	127.9	128.1	127.7	127.7	127.8
	∠(CCO′)	108.8	108.7	108.7	108.7	108.7
	∠(CO′O)	111.4	112.1	111.8	111.7	111.9
	∠(HCC)	111.4	111.3	111.5	111.4	111.7
	∠(H′CC)	109.0	108.9	108.9	108.8	108.9
	∠(H″CC)	108.9	108.6	108.6	108.7	108.3
	∠(O′OBr)	111.7	112.9	112.5	112.2	112.7
	∠(OBrO′)	110.7	112.0	110.1	111.0	109.6
	∠(HCCO)	−149.0	−147.6	−150.3	−147.6	−153.0
	∠(H′CCO)	−25.5	−25.1	−27.8	−25.2	−30.3
	∠(H″CCO)	93.1	93.4	90.5	93.3	87.7
	∠(CO′OBr)	73.7	73.9	76.2	75.9	77.5
	∠(O′OBrO′)	95.5	94.7	93.1	93.9	91.8
$CH_3COO'BrO_2$	*r*(CO)	1.218	1.210	1.210	1.207	1.207
	r(CO′)	1.341	1.343	1.341	1.344	1.347
	r(CC)	1.514	1.511	1.510	1.508	1.506
	r(CH)	1.094	1.091	1.089	1.089	1.089
	r(CH′)	1.091	1.088	1.085	1.085	1.085
	r(CH″)	1.095	1.092	1.089	1.090	1.089
	r(O′Br)	2.028	2.021	2.018	1.979	1.969
	r(BrO)	1.640	1.626	1.620	1.608	1.609
	r(BrO″)	1.640	1.624	1.618	1.608	1.608
	∠(HCC)	110.2	110.2	110.1	110.1	110.0
	∠(H′CC)	109.0	108.9	108.9	109.1	109.1
	∠(H″CC)	109.6	109.3	109.5	109.5	109.5
	∠(CCO)	125.4	125.6	125.3	125.6	125.8
	∠(CCO′)	111.9	111.4	111.8	111.6	111.5
	∠(CO′Br)	107.7	109.6	108.3	109.7	111.0
	∠(O′BrO)	97.7	97.6	97.5	97.5	97.4
	∠(O′BrO″)	111.0	102.3	102.4	102.0	101.9
	∠(HCCO)	−124.4	−126.1	−124.1	−125.0	−123.2
	∠(H′CCO)	−3.1	−4.6	−2.9	−3.6	−2.0
	∠(H″CCO)	117.3	115.7	117.7	116.9	118.7
	∠(CO′BrO)	161.6	158.2	161.2	161.4	160.9
	∠(CO′BrO″)	−84.2	−86.3	−84.4	−84.6	−85.4
CH_3COBrO_3	*r*(CBr)	2.260	2.275	2.299	2.283	2.311
	r(CC)	1.484	1.479	1.477	1.476	1.474
	r(CO)	1.167	1.157	1.154	1.155	1.152
	r(BrO)	1.658	1.645	1.639	1.626	1.629

TABLE 1 (Continued)

		levels of theory B3LYP/				
species	coordinates	6-31G(d)	6-311G(d,p)	6-311G(2d,2p)	6-311G(2df,2p)	6-311++G(3df,3pd)
CH_3COBrO_3	*r*(BrO′)	1.649	1.636	1.630	1.617	1.620
	r(CH)	1.096	1.093	1.091	1.091	1.091
	r(CH′)	1.093	1.091	1.088	1.088	1.089
	∠(CBrO)	102.8	104.1	103.9	104.2	104.7
	∠(CBrO′)	109.4	107.9	109.5	109.2	109.4
	∠(CCBr)	103.6	104.9	103.9	104.2	104.0
	∠(HCC)	108.1	108.2	108.2	108.2	108.4
	∠(H′CC)	110.0	109.5	109.4	109.6	109.3
	∠(HCH′)	111.5	111.6	111.7	111.6	111.5
	∠(OBrO′)	114.1	113.8	113.4	113.3	112.9
	∠(HCCO)	−122.0	−121.9	−121.9	−121.9	−121.7
	∠(CCBrO)	58.4	58.8	58.6	58.7	58.7

most likely CH_3COBrO_3 isomeric forms. To our knowledge, there have been no previous computational studies on any CH_3COBrO_3 species, and no experimental studies have been reported that have isolated such complexes. The CH_3COBrO_3 complex, if present in a stable form, could act as new reservoir of inorganic bromine in the stratosphere, and thus its possible existence requires investigation.

There are four types of plausible connectivities for the CH_3COBrO_3 isomers, namely (1) $CH_3COOOOBr$, (2) $CH_3COOOBrO$, (3) $CH_3COOBrO_2$, and (4) CH_3COBrO_3. In our present work, density functional theory (DFT) has been employed to examine the minimum-energy structural forms for the CH_3COBrO_3 isomers. The harmonic vibrational frequencies along with infrared intensities have been calculated to aid in the spectroscopic characterization of the CH_3COBrO_3 isomers. The heats of formation of the CH_3COBrO_3 isomers have also been estimated to determine the relative order of stability among them. Our investigation of the CH_3COBrO_3 isomeric forms should aid in providing information about the atmospheric cross-coupling chemistry between the CH_3COO_x and BrO_x radical families.

II. Computational Methods

Ab initio molecular orbital calculations were performed using the GAUSSIAN 94 program.[22] The equilibrium geometrical parameters of the CH_3COBrO_3 isomers were fully optimized, using Schlegel's method, to better than 0.001 Å for bond distances and 0.10° for bond angles with a self-consistent field (SCF) convergence of at least 10^{-9} on the density matrix. The residual root-mean-square force was less than 10^{-4} atomic units. The B3LYP (Becke's nonlocal three-parameter exchange with Lee−Yang−Parr correlation functional) method[23] was used with the 6-31G(d), 6-311G(d,p), 6-311G(2d,2p), 6-311G(2df,2p), and 6-311++G(3df,3pd) basis sets in the optimization of the structures. The vibrational frequencies and intensities of all the isomers were calculated at the B3LYP level of theory in conjugation with the 6-31G(d) and 6-311++G(3df,3pd) basis sets, using the geometrical parameters calculated at the B3LYP/6-31G(d) and B3LYP/6-311++G(3df,3pd) theory levels. The heat of formation of $CH_3COOOOBr$ was calculated using an isodesmic scheme and G2MP2 theory. The heats of formation of the other isomers were also calculated.

III. Results and Discussion

A. Structures and Vibrational Frequencies of CH_3COBrO_3 Isomers. Calculations were performed at various levels of theory to identify the lowest energy isomer on the CH_3COBrO_3 potential energy surface. Four local minimum-energy structures were located, whose optimized geometrical parameters are provided in Table 1, and structures are illustrated in Figure 1.

The ground-state geometry for $CH_3COOOOBr$ is illustrated in Figure 1a. Our computations indicate that the minimum-energy structure for $CH_3COOOOBr$ is skewed. The HCCO dihedral angle varies from 6.0° to 23.3° over the range of basis sets used, as noted from Table 1. At the B3LYP/6-311++G(3df,3pd) level of theory, the HCCO dihedral angle is 15.8°. Similar large variations are observed in the H′CCO and H″CCO dihedral angles. It is interesting to note that increasing basis set size does not show a pattern of convergence. The CO′OO dihedral angle is predicted to be 85.0°, while the O′OOBr dihedral angle is 85.1° at the B3LYP/6-311++G(3df,3pd) level of theory. A comparison can be made of the O−O and O′−O bond lengths of $CH_3COO'OOBr$ (1.355 and 1.451 Å, respectively) with the O−O and O−O′ bond lengths of the $CH_3OOO'Br$ intermediate (1.430 and 1.375 Å, respectively) formed during the CH_3O_2 + BrO reaction.[19] The bonding between the $CH_3COOOOBr$ and CH_3OOOBr species is quite similar. The O′OO angle in $CH_3COO'OOBr$ (108.6°) is narrower than the OOBr angle (112.0°) due to the greater amount of repulsion between the lone pairs of electrons on bromine with those on oxygen (comprising the −OOBr unit), compared to the repulsion occurring between the lone pairs of electrons on the two oxygen atoms (comprising the −O′OO− unit).

The second isomeric form we considered is $CH_3COOOBrO$. This, too, is a skewed structure, but with oxygen as the terminal atom (Figure 1b). The dihedral angle between the CO′OBr atoms is 77.5°, while that between the O′OBrO′ atoms is 91.8°. The OBrO′ angle (109.6°) is narrower than the O′OBr angle (112.7°). The CO′O angle in $CH_3COO'OBrO'$ (111.9°) is slightly narrower than the O′OBr angle (112.7°), due to the greater degree of repulsion between the two lone pairs of electrons on bromine with those on the oxygen atom. For different basis sets used, the O−Br bond lengths in $CH_3COO'OBrO'$ are noticeably larger than the Br−O′ bond lengths. The lone pairs of electrons on the terminal oxygen atom of $CH_3COO'OBrO'$ tend to enter into resonance with the Br−O′ bond pairs, due to which the terminal Br−O′ bond attains a partial double-bond character. Such resonance effect is not observed with the oxygen atoms that are sandwiched between the carbon and the bromine atoms. The Br−O′ bond with its partial double-bond character is, thus, shorter than the O−Br single bond. The O′−O bond length in $CH_3COO'OBrO'$ (1.422 Å) is comparable to the O−O bond length in CH_3OOBrO' (1.408 Å).[19] The O′OBr and OBrO′ angles in $CH_3COO'OBrO'$ are comparable to the OOBr and OBrO′ angles in CH_3OOBrO'.[19]

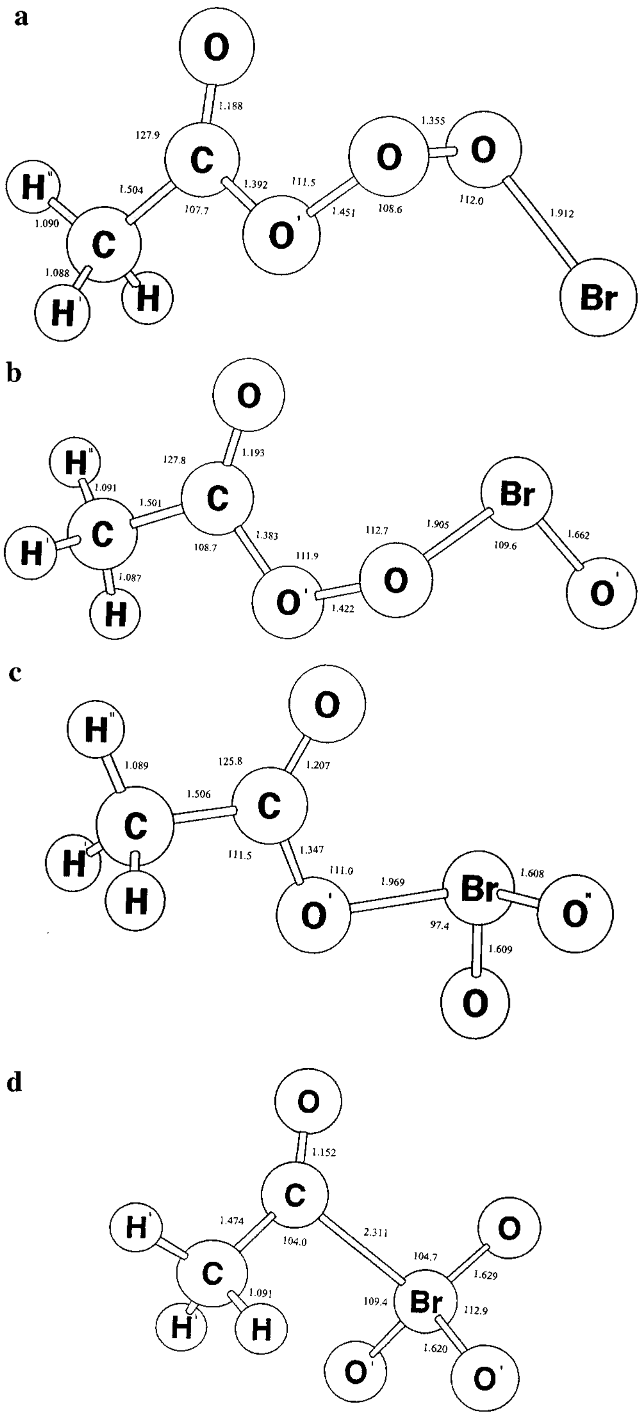

Figure 1. Minimum energy structures for the CH_3COBrO_3 isomers (a) $CH_3COOOOBr$, (b) $CH_3COOOBrO$, (c) $CH_3COOBrO_2$, and (d) CH_3COBrO_3. The values are calculated at the B3LYP/6-311++G(3df,3pd) level of theory.

The third isomeric form is $CH_3COOBrO_2$, as illustrated in Figure 1c. The O′−Br bond (1.969 Å) in $CH_3COO'BrO_2$ is longer than the bonds formed between bromine and the terminal oxygen atoms due to the participation of the lone pairs of electrons on the terminal oxygen atoms in partial resonance with their immediate bonding electron neighbors. The C−O′ bond in $CH_3COO'BrO_2$ (1.347 Å) is shorter than the C−O′ bond lengths in $CH_3COO'OOBr$ and $CH_3COO'OBrO'$, while the carbon−hydrogen bond lengths of the three species are quite similar. The O′-Br and Br−O bond lengths of $CH_3COO'BrO_2$ and $CH_3O'BrO_2$[19] are comparable. The CO′Br angle present in $CH_3COO'BrO_2$ is not present in the structures of $CH_3COO'OOBr$ and $CH_3COO'OBrO'$.

The fourth isomeric form is CH_3COBrO_3 with the three oxygen atoms forming the base of a pyramid (Figure 1d). The BrO′ bond in CH_3COBrO_3 (1.620 Å) is shorter than the terminal bromine−oxygen bonds in $CH_3COO'OOBr$ and $CH_3COO'OBrO'$, due to the strong resonance associated with the Br=O multiple bonding characteristics in CH_3COBrO_3. The Br=O bonds in CH_3COBrO_3 are slightly longer than the Br=O bonds in CH_3BrO_3 (1.612 Å).[19]

The calculated vibrational frequencies and intensities for the four isomeric forms of CH_3COBrO_3 are provided in Table 2. All isomeric forms belong to the C_1 point group. The vibrational frequencies noted in the table are obtained at the B3LYP level of theory using the 6-31G(d) and 6-311++G(3df,3pd) basis sets.

In the prediction of the vibrational frequencies of $CH_3COOOOBr$, the most intense bands appear to be the C=O and C−C stretches at 1867 and 1172 cm^{-1}, respectively, while the least intense bands appear at 3160, 3122, 532, 331, and 158 cm^{-1}. The CH_3 stretches and deformations in $CH_3COOOOBr$ occur at high frequencies. The C−C stretch occurs at a higher frequency than the O−Br stretch, consistent with the length of the C−C bond being shorter than that of the O−Br bond in $CH_3COO'OOBr$. The harmonic frequencies of $CH_3COOOOBr$ are similar to those of CH_3OOOBr.[19] However, the stretches and bends due to the presence of the −C=O group in the structure of $CH_3COOOOBr$ are absent in CH_3OOOBr. The O−Br stretch in $CH_3COO'OOBr$ (672 cm^{-1}) occurs at a slightly higher frequency than the O′-Br stretch in $CH_3OOO'Br$ (530 cm^{-1}).[19]

For $CH_3COOOBrO$, the most intense bands are predicted to be the C=O and C−C stretches occurring at 1842 and 1182 cm^{-1} respectively (similar to the most intense bands in $CH_3COOOOBr$), while the least intense bands are predicted to be the CH_3 asymmetric stretches and the OBrO′ and O′OBr bends. The C−O′ stretch in $CH_3COO'OBrO'$ (1003 cm^{-1}) occurs at a much larger frequency than the Br−O′ symmetric and asymmetric stretches (846 and 651 cm^{-1}, respectively) consistent with the C−O′ bond length being much shorter than the Br−O′ bond length. The harmonic frequencies of $CH_3COOOBrO$ are generally comparable to those of CH_3OOBrO.[19] The frequency band that may clearly distinguish $CH_3COO'OBrO'$ from $CH_3COO'OOBr$ is the O′OO bend occurring at 561 cm^{-1} in $CH_3COO'OOBr$, which is absent in the structure of $CH_3COO'OBrO'$.

The BrO symmetric and asymmetric stretches in $CH_3COOBrO_2$ (915 and 965 cm^{-1}, respectively) occur at lower frequencies than the C=O stretch (1762 cm^{-1}), consistent with the length of the terminal BrO bond being longer than the length of the C=O bond. The CO′Br bending mode in $CH_3COO'BrO_2$ (380 cm^{-1}) occurs at a higher frequency than the OBrO″ bending mode (320 cm^{-1}). The frequency modes that can clearly distinguish $CH_3COOBrO_2$ from $CH_3COO'OOBr$ are the O′−O stretch and the O′OO bend occurring in $CH_3COO'OOBr$.

The frequencies for the CH_3COBrO_3 isomeric form are also provided in Table 2. Its most intense band is the C=O stretch occurring at 2058 cm^{-1}. The C−Br stretch (492 cm^{-1}) occurs at a much lower frequency than the BrO_3 symmetric and asymmetric stretches. A frequency mode that would distinguish CH_3COBrO_3 from the $CH_3COOOOBr$ structure is the C−Br stretch in CH_3COBrO_3 that is absent in $CH_3COOOOBr$.

B. Relative Energetics of CH_3COBrO_3 Isomers. The calculated total and relative energies for the four minimum-energy isomers of CH_3COBrO_3 are presented in Table 3. The total energies for the reactants and products of the CH_3COO_2

TABLE 2: Harmonic Frequencies (cm^{-1}) and Intensities ($km\ mol^{-1}$) of CH_3COBrO_3 Isomers

			B3LYP/6-31G(d)		B3LYP/6-311++G(3df,3pd)	
species	mode no.	mode description	freq	int	freq	int
$CH_3COO'OOBr$	1	CH_3 asymmetric stretch	3184	2	3160	2
	2	CH_3 asymmetric stretch	3144	2	3122	2
	3	CH_3 symmetric stretch	3076	0	3056	0
	4	$C=O$ stretch	1895	250	1867	289
	5	CH_3 asymm. deformation	1501	11	1477	11
	6	CH_3 asymm. deformation	1498	12	1470	11
	7	CH_3 symm. deformation	1418	22	1397	21
	8	CC stretch	1193	289	1172	270
	9	CH_3 rock	1073	7	1062	7
	10	CO' stretch	998	33	993	35
	11	OO stretch	938	72	928	68
	12	CO' stretch	850	54	838	73
	13	$O'O$ stretch	725	91	720	90
	14	OBr stretch	672	3	672	6
	15	$CO'O$ bend	593	3	598	4
	16	$O'OO$ bend	557	18	561	13
	17	CH_3 twist	524	2	532	2
	18	OOBr bend	411	15	414	11
	19	H-wag	329	2	331	1
	20	CH_3 twist	194	0	196	0
	21	torsion	156	0	158	1
	22	torsion	78	2	78	3
	23	torsion	56	0	59	0
	24	torsion	30	1	37	0
$CH_3COO'OBrO'$	1	CH_3 asymmetric stretch	3182	2	3158	1
	2	CH_3 asymmetric stretch	3146	2	3124	1
	3	CH_3 symmetric stretch	3074	0	3055	0
	4	$C=O$ stretch	1862	174	1842	211
	5	CH_3 asymm. deformation	1502	8	1478	8
	6	CH_3 asymm. deformation	1497	15	1470	14
	7	CH_3 symm. deformation	1422	24	1400	21
	8	CC stretch	1208	280	1182	266
	9	CH_3 rock	1072	11	1061	9
	10	CO' stretch	1011	38	1003	35
	11	$O'O$ stretch	912	56	889	33
	12	CC stretch	862	33	849	74
	13	BrO' symmetric stretch	842	84	846	96
	14	BrO' asymmetric stretch	654	15	651	16
	15	OBr symmetric stretch	601	7	611	6
	16	OBr asymmetric stretch	485	11	497	15
	17	$O'OBr$ bend	428	2	433	2
	18	$OBrO'$ bend	333	1	338	1
	19	torsion	262	6	271	7
	20	H-wag	183	5	192	4
	21	CH_3 twist	103	10	103	8
	22	torsion	97	2	82	3
	23	torsion	70	1	61	8
	24	torsion	61	6	53	0
$CH_3COO'BrO_2$	1	CH_3 asymmetric stretch	3183	3	3161	2
	2	CH_3 asymmetric stretch	3144	3	3120	1
	3	CH_3 symmetric stretch	3075	2	3056	1
	4	$C=O$ stretch	1773	201	1762	243
	5	CH_3 asymm. deformation	1499	10	1473	10
	6	CH_3 symm. deformation	1496	17	1470	18
	7	CH_3 symm. deformation	1412	10	1393	14
	8	CC stretch	1257	276	1219	298
	9	CH_3 rock	1076	8	1069	7
	10	CH_3 rock	1006	23	995	39
	11	BrO asymmetric stretch	948	87	965	121
	12	BrO symmetric stretch	931	11	915	24
	13	BrO'' stretch	890	70	913	95
	14	$O'Br$ stretch	675	70	679	79
	15	$O'BrO$ bend	603	6	607	5
	16	$O'BrO''$ bend	483	12	493	20
	17	$CO'Br$ bend	358	19	380	18
	18	$OBrO''$ bend	308	43	320	49
	19	CH_3 twist	242	5	255	6
	20	CH_3 twist	227	4	236	6
	21	H-wag	131	6	132	7
	22	torsion	94	2	93	3
	23	torsion	72	0	71	0
	24	torsion	66	4	61	4

TABLE 2 (Continued)

			B3LYP/6-31G(d)		B3LYP/6-311++G(3df,3pd)	
species	mode no.	mode description	freq	int	freq	int
CH_3COBrO_3	1	CH_3 asymmetric stretch	3172	2	3142	3
	2	CH_3 asymmetric stretch	3143	7	3115	9
	3	BrO_3 asymmetric stretch	3066	7	3041	10
	4	C=O stretch	2045	429	2058	499
	5	BrO_3 asymm. stretch	1480	8	1452	6
	6	CH_3 symm. stretch	1469	26	1441	21
	7	BrO_3 symm. stretch	1401	38	1382	28
	8	CH_3 asymm. deformation	1090	180	1067	176
	9	CH_3 symm. deformation	1054	2	1043	2
	10	CC stretch	914	23	916	105
	11	BrO_3 rock	897	90	906	37
	12	CH_3 asymm. deformation	883	96	898	129
	13	BrO stretch	806	71	831	99
	14	CBr stretch	503	86	492	106
	15	BrO_3 asymm. deformation	462	0	462	0
	16	BrO_3 asymm. deformation	376	86	394	113
	17	CH_3 rock	329	14	346	17
	18	BrO_3 rock	312	13	336	13
	19	BrO_3 symm. deformation	264	3	255	2
	20	CO ip bend	205	34	187	53
	21	CO op bend	180	1	163	0
	22	CCBr deformation	103	1	97	2
	23	torsion	98	2	89	2
	24	torsion	43	4	29	4

+ BrO reaction are also provided in the table. Using the B3LYP level of theory and the 6-31G(d), 6-311G(d,p), 6-311G(2d,2p), and 6-311G(2df,2p) basis sets, the order of decreasing relative stability among the isomers is $CH_3COOOOBr > CH_3COOBrO_2 > CH_3COOOBrO > CH_3COBrO_3$, indicating that the $CH_3COOOOBr$ structural form possesses the least energy, while the CH_3COBrO_3 structural form possesses the most energy. However, when the large 6-311++G(3df,3pd) basis set is used, the order of energies changes, and the order of decreasing stability among the isomers becomes $CH_3COOBrO_2 > CH_3COOOOBr > CH_3COOOBrO > CH_3COBrO_3$. The order of energies at the B3LYP/6-311++G(3df,3pd) theory level matches the order of energies calculated using the G2MP2 theory. Previous studies conducted by Guha and Francisco on the isomers of $HBrO_3$[16] and CH_3BrO_3[19] have shown that G1 and G2 theories are more reliable in predicting the correct order of energies than the B3LYP level of theory. Thus, for the CH_3COBrO_3 isomers, we believe that the order of energies predicted by the G2MP2 theory is reasonable. The increased stability of $CH_3COOBrO_2$ over $CH_3COOOOBr$ is similar to the pattern of stability observed in $HOBrO_2$ over HOOOBr[16] and CH_3OBrO_2 over CH_3OOOBr.[19] For all the $XBrO_3$ (X = H, CH_3, and CH_3CO) isomers, the same pattern of inversion in stability is found, i.e., the $XOBrO_2$ (X = H, CH_3, and CH_3CO) form becomes the most stable, with the incorporation of the B3LYP level of theory combined with a very large basis set (and further, the G2 theory). Such an observation points to the limitation of the B3LYP theory level in conjugation with small and medium-sized basis sets in predicting the correct order of stability among the various isomeric forms that display hypervalent character.

The relative energetic stability among the CH_3COBrO_3 isomers is sensitive to the type of basis sets used to perform the calculations. For instance, the relative energy difference between $CH_3COOOOBr$ and $CH_3COOBrO_2$ at the B3LYP/6-311G(d,p) level of theory is 15.9 kcal mol^{-1}. However, using the large 6-311++G(3df,3pd) basis set, the relative energy difference between the two structures decreases markedly to −1.6 kcal mol^{-1}.

An isodesmic reaction scheme is used to estimate the heat of formation of $CH_3COOOOBr$ using G2MP2 and B3LYP energetics. Isodesmic reactions, which have been typically used to obtain the heats of formation for many molecules, are those in which the reactants and products contain the same types of bonds, i.e., the number of bonds broken and formed is conserved. The isodesmic reaction scheme requires that the heats of formation of all the molecules involved in the reaction be known, with the exception of the heat of formation of the particular isomer. Because of this property, errors in the energy that might occur due to defects in the basis set and electron correlation cancel, to a large extent. The isodesmic scheme used here is $CH_3COOOOBr + 3H_2O \rightarrow CH_3COOH + 2HOOH + HOBr$. During the calculation of the heat of formation of $CH_3COOOOBr$ using the isodesmic scheme, literature values for the heats of formation of H_2O (-57.10 ± 0.10 kcal mol^{-1}),[24] HOOH (-31.02 ± 0.05 kcal mol^{-1}),[24] CH_3COOH (99.97 kcal mol^{-1}),[25] and HOBr (−10.93 kcal mol^{-1})[24] were used. Using these results, we were able to calculate the heats of reaction for the isodesmic scheme and the heats of formation of $CH_3COOOOBr$ at various levels of theory (refer to Table 4).

For $CH_3COOOOBr$, the heat of formation is predicted to be −23.0 kcal mol^{-1} at the B3LYP level of theory, using the large 6-311++G(3df,3pd) basis set and −30.5 kcal mol^{-1} using the G2MP2 theory. Using the relative energies of the CH_3COBrO_3 isomers listed in Table 3 along with the heat of formation of $CH_3COOOOBr$ determined using the isodesmic scheme, we obtained values of −11.0, −24.6, and 35.4 kcal mol^{-1} as the heats of formation for $CH_3COOOBrO$, $CH_3COOBrO_2$, and CH_3COBrO_3, respectively, at the B3LYP/6-311++G(3df,3pd) theory level (refer to Table 5). Using G2MP2 theory, the heats of formation for $CH_3COOOBrO$, $CH_3COOBrO_2$, and CH_3COBrO_3 were obtained as −21.6, −38.2, and 18.1 kcal mol^{-1}, respectively. Both the B3LYP/6-311++G(3df,3pd) and G2MP2 analyses provided here suggest that the lowest heat of formation is possessed by the $CH_3COOBrO_2$ isomer. The $CH_3COOOOBr$ structural form has a higher heat of formation than the $CH_3COOBrO_2$ structure by 7.7 kcal mol^{-1}, using the G2MP2 theory. The $CH_3COOOBrO$ and CH_3COBrO_3 structural forms possess higher heats of formation than $CH_3COOBrO_2$ by 16.6 and 56.3 kcal mol^{-1}, respectively, using the G2MP2 theory. The CH_3COBrO_3 structure possesses the highest heat of

TABLE 3: Total and Relative Energies of CH_3COBrO_3 Isomers and Total Energies (kcal mol^{-1}) of Reactants and Products of the CH_3COO_2 + BrO Reaction

Total and Relative Energies of CH_3COBrO_3 Isomers

	species			
levels of theory	$CH_3COOOOBr$	$CH_3COOOBrO$	$CH_3COOBrO_2$	CH_3COBrO_3
		Total Energies (hartrees)		
B3LYP/6-31G(d)	−2950.40577	−2950.37537	−2950.38250	−2950.27521
B3LYP/6-311G(d,p)	−2952.95432	−2952.92008	−2952.92874	−2952.82701
B3LYP/6-311G(2d,2p)	−2952.96621	−2952.93662	−2952.94902	−2952.84664
B3LYP/6-311G(2df,2p)	−2952.97897	−2952.95399	−2952.97412	−2952.87590
B3LYP/6-311++G(3df,3pd)	−2952.99822	−2952.97869	−2953.00052	−2952.90327
G2MP2	−2950.76918	−2950.75457	−2950.78111	−2950.68984
		Relative Energies (kcal mol^{-1})[a]		
B3LYP/6-31G(d)	0.0	18.8	14.4	80.7
B3LYP/6-311G(d,p)	0.0	21.2	15.9	78.7
B3LYP/6-311G(2d,2p)	0.0	18.3	10.6	73.8
B3LYP/6-311G(2df,2p)	0.0	15.4	2.8	63.5
B3LYP/6-311++G(3df,3pd)	0.0	12.0	−1.6	58.4
G2MP2	0.0	8.9	−7.7	48.6

Total Energies (kcal mol^{-1}) of Reactants and Products of the CH_3COO_2 + BrO Reaction

	species										
levels of theory	CH_3COO_2	BrO	CH_3COOBr	O_2	CO_2	CH_3Br	CH_3COBr	O_3	CH_3	OBrO	CH_3OOBr
B3LYP/6-31G(d)	−303.55609	−2646.81083	−2800.12751	−150.25742	−188.58094	−2611.61668	−2724.95440	−225.40645	−39.83829	−2721.93811	−2761.91580
B3LYP/6-311G(d,p)	−303.64393	−2649.27505	−2802.63303	−150.30260	−188.64114	−2614.07350	−2727.44116	−225.47079	−39.85376	−2724.42181	−2764.41167
B3LYP/6-311G(2d,2p)	−303.65443	−2649.27711	−2802.63894	−150.30685	−188.64534	−2614.07133	−2727.44260	−225.48033	−39.85602	−2724.43334	−2764.41697
B3LYP/6-311G(2df,2p)	−303.66219	−2649.28302	−2802.64840	−150.31084	−188.65223	−2614.07399	−2727.44826	−225.48637	−39.85638	−2724.44777	−2764.42410
B3LYP/6-311++G(3df,3pd)	−303.67442	−2649.29460	−2802.66414	−150.31815	−188.66040	−2614.08076	−2727.45996	−225.49798	−39.85836	−2724.46620	−2764.43761
G2MP2	−303.13378	−2647.59140	−2800.66309	−150.09959	−188.35662	−2612.38262	−2725.57014	−225.16707	−39.74391	−2722.65917	−2762.51168

[a] Corrected for zero-point energies using B3LYP/6-31G(d) frequencies.

TABLE 4: Isodesmic Heats of Reaction[a] (kcal mol^{-1}) and Heats of Formation[a] (kcal mol^{-1}) of $CH_3COOOOBr$

levels of theory	H_2O	CH_3COOH	HOBr	HOOH	$CH_3COOOOBr$	$H°_{r,0}$ $CH_3COOOOBr + 3H_2O \rightarrow CH_3COOH + 2HOOH + HOBr$	$H°_{f,0}$ $CH_3COOOOBr$
B3LYP/6-31G(d)	−76.40895	−229.08178	−2647.46501	−151.53321	−2950.40577	16.3	−17.9
B3LYP/6-311G(d,p)	−76.44745	−229.15643	−2649.93714	−151.59185	−2952.95432	16.3	−17.9
B3LYP/6-311G(2d,2p)	−76.45212	−229.16465	−2649.93917	−151.59908	−2952.96621	14.1	−15.7
B3LYP/6-311G(2df,2p)	−76.45276	−229.17005	−2649.94379	−151.60137	−2952.97897	17.1	−18.7
B3LYP/6-311++G(3df,3pd)	−76.46451	−229.18157	−2649.95629	−151.61319	−2952.99822	21.4	−23.0
G2MP2	−76.33001	−228.74759	−2648.24947	−151.36133	−2950.76918	28.9	−30.5

[a] Corrected for zero-point energies using B3LYP/6-31G(d) frequencies.

TABLE 5: Heats of Formation[a] (kcal mol^{-1}) of CH_3COBrO_3 Isomers

species	B3LYP/6-311++G(3df,3pd)	G2MP2
$CH_3COOOOBr$	−23.0	−30.5
$CH_3COOOBrO$	−11.0	−21.6
$CH_3COOBrO_2$	−24.6	−38.2
CH_3COBrO_3	35.4	18.1

[a] Corrected for zero-point energies using B3LYP/6-31G(d) frequencies.

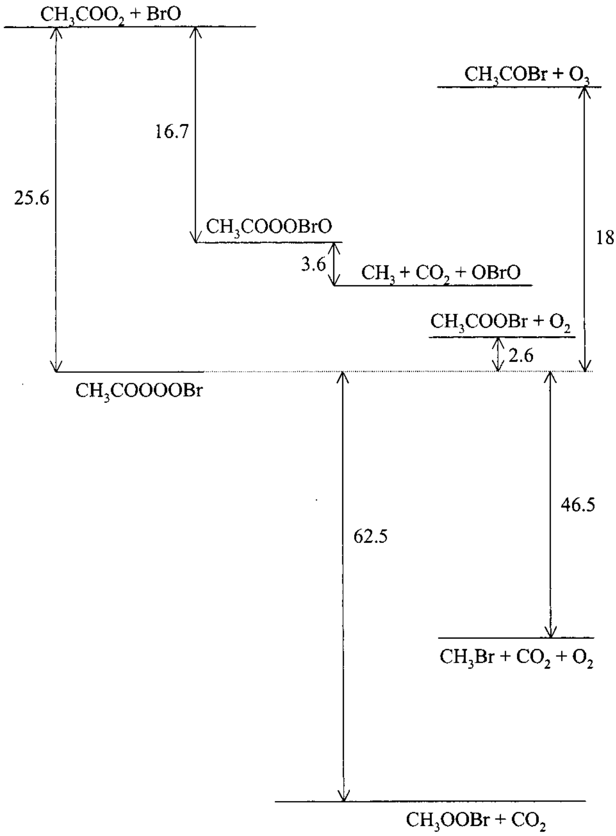

Figure 2. Energetics of the formation and dissociation of $CH_3COOOOBr$ and $CH_3COOOBrO$. The values are calculated using the G2MP2 theory.

formation andthe least stability. It is interesting to note that although the B3LYP/6-311++G(3df,3pd) and G2MP2 levels of theory predict the same relative energetic ordering of the CH_3COBrO_3 isomers, the G2MP2 theory level predicts the individual isomers to be more stable than that predicted by the B3LYP density functional theory.

The heats of reaction for the formation and dissociation of the $CH_3COOOOBr$ and $CH_3COOOBrO$ isomers from the reaction between CH_3COO_2 and BrO radicals are listed in Table 6. Using G2MP2 theory, the heat of reaction for the formation of $CH_3COOOOBr$ is −25.6 kcal mol^{-1}, while the heat of reaction for the dissociation of $CH_3COOOOBr$ into $CH_3COOBr + O_2$, $CH_3OOBr + CO_2$, $CH_3Br + CO_2 + O_2$, and $CH_3COBr + O_3$ are 2.6, −62.5, −46.5, and 18.4 kcal mol^{-1}, respectively. The formation of the $CH_3COOOBrO$ isomer from the reaction between CH_3COO_2 and BrO radicals possesses a heat of reaction of −16.7 kcal mol^{-1}, while the dissociation of $CH_3COOOBrO$ into $CH_3 + CO_2 + OBrO$ requires a heat of reaction of −3.6 kcal mol^{-1}, at 0 K (using the G2MP2 theory).

The energetics of the formation and dissociation of $CH_3COOOOBr$ and $CH_3COOOBrO$ is illustrated in Figure 2. The CH_3COO_2 + BrO reaction is most likely to proceed via the formation of the $CH_3COOOOBr$ isomer. Thermodynamic

TABLE 6: Heats of Reaction[a] (kcal mol^{-1}) for the Formation and Dissociation of $CH_3COOOOBr$ and $CH_3COOOBrO$

	$H^\circ_{r,0}$						
levels of theory	$CH_3COO_2 + BrO \rightarrow CH_3COOOOBr$	$CH_3COOOOBr \rightarrow CH_3COOBr + O_2$	$CH_3COOOOBr \rightarrow CH_3OOBr + CO_2$	$CH_3COOOOBr \rightarrow CH_3Br + CO_2 + O_2$	$CH_3COOOOBr \rightarrow CH_3COBr + O_3$	$CH_3COO_2 + BrO \rightarrow CH_3COOOBrO$	$CH_3COOOBrO \rightarrow CH_3 + CO_2 + OBrO$
B3LYP/6-31G(d)	−22.4	11.6	−57.4	−33.6	26.5	−3.6	4.5
B3LYP/6-311G(d,p)	−20.2	10.2	−62.1	−42.3	24.9	1.0	−4.7
B3LYP/6-311G(2d,2p)	−19.8	11.3	−60.6	−38.8	25.5	−1.5	−5.6
B3LYP/6-311G(2df,2p)	−19.2	10.9	−61.4	−39.3	26.1	−3.8	−5.3
B3LYP/6-311++G(3df,3pd)	−16.3	8.5	−62.9	−41.1	23.6	−4.4	−2.9
G2MP2	−25.6	2.6	−62.5	−46.5	18.4	−16.7	−3.6

[a] Corrected for zero-point energies using B3LYP/6-31G(d) frequencies.

considerations suggest that $CH_3OOBr + CO_2$ could be formed as byproducts of the dissociation of $CH_3COOOOBr$ with an enthalpy of -62.5 kcal mol^{-1}. The formation of $CH_3Br + CO_2 + O_2$ is also thermodynamically feasible from the dissociation of the $CH_3COOOOBr$ isomer. If the $CH_3COOOBrO$ isomer is formed from the CH_3COO_2 + BrO reaction, it will probably dissociate to produce CH_3, CO_2, and OBrO. The pathways of formation of CH_3Br (an important source of bromine atoms) and OBrO (the principle bromine species at mid-latitudes during the nighttime, and a catalyst for ozone destruction during the daytime) from the dissociation of $CH_3COOOOBr$ and $CH_3COOOBrO$, respectively, are important in the atmospheric context.

IV. Conclusion

The equilibrium structures, vibrational spectra, relative energetics, and heats of formation of the CH_3COBrO_3 isomers have been investigated with density functional and *ab initio* methods. The $CH_3COOBrO_2$ structural form was found to be the most stable among the isomers with an estimated heat of formation of -38.2 kcal mol^{-1}. The heats of formation of $CH_3COOOOBr$, $CH_3COOOBrO$, and CH_3COBrO_3 were determined as -30.5, -21.6, and 18.1 kcal mol^{-1}, respectively. The reaction between CH_3COO_2 and BrO radicals could proceed via the formation of $CH_3COOOOBr$ and $CH_3COOOBrO$ as complex intermediates. If $CH_3COOOOBr$ is formed, it will, most likely, dissociate to produce either CH_3OOBr and CO_2 or CH_3Br, CO_2, and O_2 as the possible byproducts. If, on the other hand, $CH_3COOOBrO$ is formed as an intermediate, is will probably dissociate to produce CH_3, CO_2, and OBrO.

References and Notes

(1) Anderson, J. G.; Toohey, D. W.; Brune, W. H. *Science* **1991**, *251*, 39.

(2) Salawitch, R. J.; McElroy, M. B.; Yatteau, J. H.; Wofsy, S. C.; Schoeberl, M. R.; Lait, L. R.; Newman, P. A.; Chan, K. R.; Loewenstein, M.; Podolske, J. R.; Strahan, S. E.; Proffitt, M. H. *Geophys. Res. Lett.* **1990**, *17*, 561.

(3) Yung, Y. L.; Pinto, J. P.; Watson, R. T.; Sander, S. P. *J. Atmos. Sci.* **1980**, *37*, 339.

(4) WMO. *Scientific Assessment of Ozone Depletion*; National Aeronautics and Space Administration, 1994.

(5) Cox, R. A.; Sheppard, D. W. *J. Chem. Soc., Faraday Trans. 2* **1982**, *78*, 1383.

(6) Baulch, D. L.; Cox, R. A.; Hampton, R. F., Jr.; Kerr, J. A.; Troe, J.; Watson, R. T. *J. Phys. Chem. Ref. Data* **1980**, *9*, 295.

(7) Poulet, G.; Pirre, M.; Maguin, F.; Ramaroson, R.; Le Bras, G. *Geophys. Res. Lett.* **1992**, *19*, 2305.

(8) Hayman, G. D.; Danis, F.; Thomas, D. H. J. Peeters, Air Pollution Report, No. 45, Commission of the European Communities, Brussels, 1993.

(9) Bridier, I.; Veyret, B.; Lesclaux, R. *Chem. Phys. Lett.* **1993**, *201*, 563.

(10) Larichev, M.; Maguin, F.; Le Bras, G.; Poulet, G. *J. Phys. Chem.* **1995**, *99*, 15911.

(11) Elrod, M. J.; Meads, R. F.; Lipson, J. B.; Seeley, J. V.; Molina, M. J. *J. Phys. Chem.* **1996**, *100*, 5808.

(12) Cronkhite, J. M.; Stickel, R. E.; Nicovich, J. M.; Wine, P. H. *J. Phys. Chem. A* **1998**, *102*, 6651.

(13) Mellouki, A.; Talukdar, R. K.; Howard, C. J. *J. Geophys. Res.* **1994**, *99*, 22949.

(14) Garcia, R. R.; Solomon, S. *J. Geophys. Res.* **1994**, *99*, 12937.

(15) Li. Z.; Friedl, R. R.; Sander, S. P. *J. Chem. Soc., Faraday Trans.* **1997**, *93*, 2683.

(16) Guha, S.; Francisco, J. S. *J. Phys. Chem. A* **1998**, *102*, 2072.

(17) Guha, S.; Francisco, J. S. *J. Phys. Chem. A* **1999**, *103*, 8000.

(18) Aranda, A.; Le Bras, G.; La Verdet, G.; Poulet, G. *Geophys. Res. Lett.* **1997**, *24*, 2745.

(19) Guha, S.; Francisco, J. S. *J. Phys. Chem. A*, **2000**, *104*, 3239.

(20) Moortgat, G. K.; Cox, R. A.; Schuster, G.; Burrows, J. P.; Tyndall, G. S. *J. Chem. Soc., Faraday Trans. 2* **1989**, *85*, 809.

(21) Maricq, M. M.; Shi, J.; Szente, J. J.; Rimai, L.; Kaiser, E. W. *J. Phys. Chem.* **1993**, *97*, 9686.

(22) Frisch, M. J.; Trucks, G. W.; Schlegel, H. B.; Gill, P. M. W.; Johnson, B. G.; Robb, M. A.; Cheeseman, J. R.; Keith, T.; Petersson, G. A.; Montgomery, J. A.; Raghavachari, K.; Al-Laham, M. A.; Zakrzewski, V. G.; Ortiz, J. V.; Foresman, J. B.; Cioslowski, J.; Stefanov, B. B.; Nanayakkara, A.; Challacombe, M.; Peng, C. Y.; Ayala, P. Y.; Chen, W.; Wong, M. W.; Andres, J. L.; Replogle, E. S.; Gomperts, R.; Martin, R. L.; Fox, D. J.; Binkley, J. S.; Defrees, D. J.; Baker, J.; Stewart, J. P.; Head-Gordon, M.; Gonzalez, C.; Pople, J. A. *Gaussian 94*, revision D.2; Gaussian, Inc.: Pittsburgh, PA, 1995.

(23) Lee, C.; Yang, W.; Parr, R. G. *Phys. Rev. B* **1988**, *41*, 785.

(24) Chase, M. W.; Davies, C. A.; Downey, J. R.; Frurip, D. J.; McDonald, R. A.; Syverud, A. N. *J. Phys. Chem. Ref. Data, Suppl. 1*, **1985**.

(25) Wagman, D. D.; Evans, W. H.; Parker, V. B.; Schumm, R. H.; Halow, I.; Bailey, S. M.; Churney, K. L.; Nuttall, R. C. *J. Phys. Chem. Ref. Data, Suppl. 2*, **1982**.